Finite-size effect on the Raman spectra of carbon nanotubes

doi: 10.1103/PhysRevB.59.2388

Finite-size effect on the Raman spectra of carbon nanotubes

R. Saito, T. Takeya, and T. Kimura
Department of Electronics Engineering, University of Electro-Communications, Chofu, 182-8585 Tokyo, Japan

G. Dresselhaus
Francis Bitter Magnet Laboratory, Massachusetts Institute of Technology, Cambridge, Massachusetts 02139

M. S. Dresselhaus
Department of Electrical Engineering and Computer Science, Department of Physics, Massachusetts Institute of Technology, Cambridge, Massachusetts 02139

(Received 6 August 1998)

Using nonresonant bond polarization theory, we have calculated the Raman intensity of a single-wall carbon nanotube of finite length. The calculations show that the Raman peaks in the intermediate frequency range ($500-1200\ \mathrm{cm}^{-1}$) have no intensity for infinite nanotubes, but do have some intensity for finite nanotubes. These intermediate frequency modes, which are sensitive to the nanotube length, correspond to vibrations along the nanotube axis. We also found an edge state of the breathing phonon mode at an open end of the carbon nanotube, which is Raman active. [S0163-1829(99)08603-8]

I. INTRODUCTION

Carbon nanotubes of finite length have become an important subject for nanotube physics, especially in connection with the single-wall carbon nanotube field-effect transistor, TUBEFET.[1] In a previous paper, we have calculated Raman intensities for an infinite length single-wall carbon nanotube as a function of chirality and diameter within the nonresonant, bond polarization model.[2] Specifically, we have reported Raman intensities in the low-frequency (below $500\ \mathrm{cm}^{-1}$) and the high-frequency regions (between $1550-1650\ \mathrm{cm}^{-1}$). Among the low-frequency modes, the strong Raman-active radial breathing mode with A_{1g} symmetry is a mode that is special for the nanotube geometry, and the frequency of this mode has been used to assign (n,m) indices to the nanotube, since the frequency of the radial breathing mode is inversely proportional to the nanotube diameter.[2] Higher-frequency Raman-active modes of a carbon nanotube originate from the E_{2g_2} Raman mode of graphite, which as a result of zone-folding splits into A_{1g}, E_{1g}, and E_{2g} modes in the symmetry of the nanotube. Kasuya *et al.*[3] and Pimenta *et al.*[4,5] have reported a diameter dependence of the high-frequency modes that arises from the zone folding of the phonon dispersion relations of 2D graphite in the circumferential direction of the nanotube. As for the modes with intermediate frequencies, no Raman peaks were found in the previous calculation,[2] although the experiments reported weak peaks at intermediate frequencies between 500 to $1200\ \mathrm{cm}^{-1}$.[6] In this paper we consider the reason why previous calculations did not obtain any Raman intensity for this intermediate frequency region.

The group theory for carbon nanotubes predicts that there are 15 or 16 zone-center Raman-active modes for all armchair (n,n), zigzag $(n,0)$, and chiral (n,m) $(n\neq m)$ nanotubes.[7,8] Armchair and zigzag nanotubes have mirror symmetry along the nanotube axis taken in the z direction, and we hereafter call these tubes ''achiral nanotubes.'' The irreducible representations of the Raman-active modes correspond to $\{A_{1g},E_{1g},E_{2g}\}$ or $\{A_g,E_1,E_2\}$ vibrational modes for achiral or chiral nanotubes, respectively. The corresponding basis functions of the representations $\{A_{1g}$, E_{1g}, and $E_{2g}\}$ are x^2+y^2, $\{xz,yz\}$, and $\{x^2-y^2,xy\}$, for which the amplitudes of the vibrations have zero, two, and four nodes in the xy plane, respectively. Since there are two carbon atoms in the 2D unit cell of the hexagonal lattice, the graphene phonon modes consist of either in-phase or out-of-phase vibrations for which the two atoms vibrate in the same or in opposite directions, respectively. The in-phase and out-of-phase Raman modes correspond to the low- and high-frequency regions, respectively. Further, because of the anisotropy of the graphitic plane, the in-plane mode has a higher frequency than the out-of-plane modes. Thus the graphene phonon modes are divided into in-phase or out-of-phase modes, and into in-plane or out-of-plane modes.

Correspondingly, for the intermediate frequency modes for carbon nanotubes, which are obtained from zone folding of the 2D graphite phonon dispersion relations, nanotubes have ''in-phase-and-in-plane'' and ''out-of-phase-and-out-of-plane'' modes. In this paper we show that the A_{1g} mode whose polarization is parallel to the z axis is relevant to the weak Raman intensity observed in the intermediate frequency region. This breathing mode in the z direction should be silent for an infinite nanotube, since there is no end to be polarized in this case. A Raman-active z-direction breathing mode should, however, be possible for finite nanotubes of finite length, and this result is confirmed in this paper.

The synthesis of single-wall carbon nanotubes (SWCN's) is now successful with high yield using either the laser ablation method[9,10] or the arc discharge method[11] with transition metal catalysts, in which a bundle of SWCN's forms a triangular lattice of nanotubes, known as a *rope*.[9,10] Although the nanotubes are aligned in the rope sample, the nanotubes in the rope are not always straight nor infinitely long. Thus the

nanotube bending and the presence of nanotube ends should affect the polarization caused by the laser light in the Raman experiment. In order to understand this effect, we have in the present paper calculated the Raman intensity for a nanotube of finite length. We find that the intermediate frequency Raman modes are ascribed to the nanotube end polarized modes. Furthermore, we found an edge state of a phonon mode in the intermediate-frequency region, which is also Raman-active.

In Sec. II we briefly explain the method for calculating the Raman intensity, and in Sec. III the calculated Raman intensities for different chiral nanotubes are presented for nanotubes with different lengths. Finally a summary of the findings is given in Sec. IV.

II. METHOD

The phonon modes for a nanotube of finite length are obtained by tight-binding molecular dynamics (TBMD), which we have previously used for a periodic system.[2] For simplicity we use the same atomic force constant parameters that are used to calculate the phonon modes in the periodic system.[2,6,12] The number of carbon atoms in the calculation becomes large in the case of a finite nanotube compared with that in the periodic case. By solving the dynamic matrix once, we get all the phonon modes. Because of the lower symmetry of the finite system relative to the periodic system, many Raman-active modes are possible from group theoretical considerations. Using the same bond polarization parameters that we used in the previous paper,[2] we simply calculate the Raman intensity for all phonon modes for the case of a nanotube of finite length.

In the present calculation, we consider only the case of a (10,10) armchair nanotube. According to the previous calculation, there is no chiral angle dependence of the Raman intensity, but the frequencies depend only on the tube diameter.[2] Nanotubes of up to 20T are considered in the calculation, where T is the translation vector for the (10,10) nanotube.[7,8] Using the same notation as for the (10,10) chiral vector, the translation vector is expressed by $(1,-1)$. The actual length of 20T corresponds to 49.2 Å. Although most of the single-wall carbon nanotubes observed in the rope are much longer than this length, we can see the effect of the finite size of the nanotube on the Raman intensity even for such a small length. For a 20T length and the corresponding 800 atoms for a (10,10) nanotube, the Raman intensity of 2400 phonon modes are directly calculated in this work. As for the edges, we simply cut the nanotube in the computer so that open ends without any terminations are used in the calculation.

The Raman-active modes in the carbon nanotubes are calculated at a phonon temperature of 300 K, which appears in the formula for the Bose distribution function for phonons. We consider two configurations (VV and VH) for the polarized light, in which the incident and scattered polarizations are parallel and perpendicular to each other for the VV and VH configurations, respectively. As for the orientation of the nanotube axis, we consider a random distribution of nanotube axes, for which the Raman intensities of the nanotubes along various directions are averaged out.

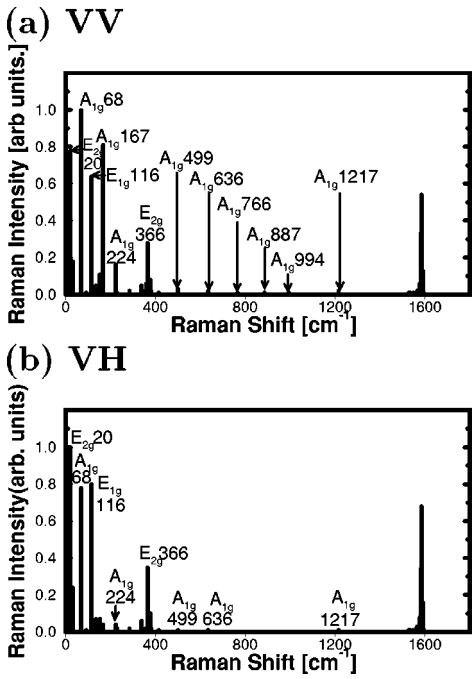

FIG. 1. Calculated Raman intensities for a 20T (10,10) nanotube for (a) VV and (b) VH configuration of polarizations.

III. CALCULATED RESULTS FOR THE RAMAN INTENSITY

In Fig. 1, we show the calculated Raman intensities for the (10,10) armchair nanotubes of 20T length. Figures 1(a) and 1(b) correspond to the VV and VH configurations for the polarized light, respectively. The Raman intensity is normalized to unity for the maximum intensity for each configuration. The ratio of the maximum intensity of the VV polarization to that of the VH polarization is about the same order of magnitude (~ 0.6) for (10,10) armchair nanotubes of different lengths.

Because of the symmetry lowering of the nanotube due to finite-size effects, many Raman-active modes appear in both polarization configurations, as shown in Fig. 1. In particular, we can see some A_{1g} modes in the intermediate frequency region between 500 to 1000 cm^{-1} and at 1217 cm^{-1}, which were silent (had essentially zero intensity) in the case of infinite nanotubes.[2] Although the intensity of these intermediate Raman modes are relatively weak compared with the lower- and higher-frequency modes, the appearance of the peaks comes from the finite-size effect, which we will show below.

When we examine the normal mode displacements associated with the A_{1g} modes, these modes consist of (1) r breathing modes whose vibrations are in the radial direction, and (2) z breathing modes whose vibrations are along the nanotube axis. The r breathing modes appear in the lower-frequency region, since we see the breathing mode in the infinite nanotube. The z breathing modes appear mainly in the intermediate-frequency region. The z breathing modes should be silent for the infinite nanotube, because of the absence of polarization of the molecule along the z axis for a nanotube without any ends. Among the A_{1g} modes shown in Fig. 1, the modes at 153, 157, 166, 167, 183, and 211 cm^{-1}

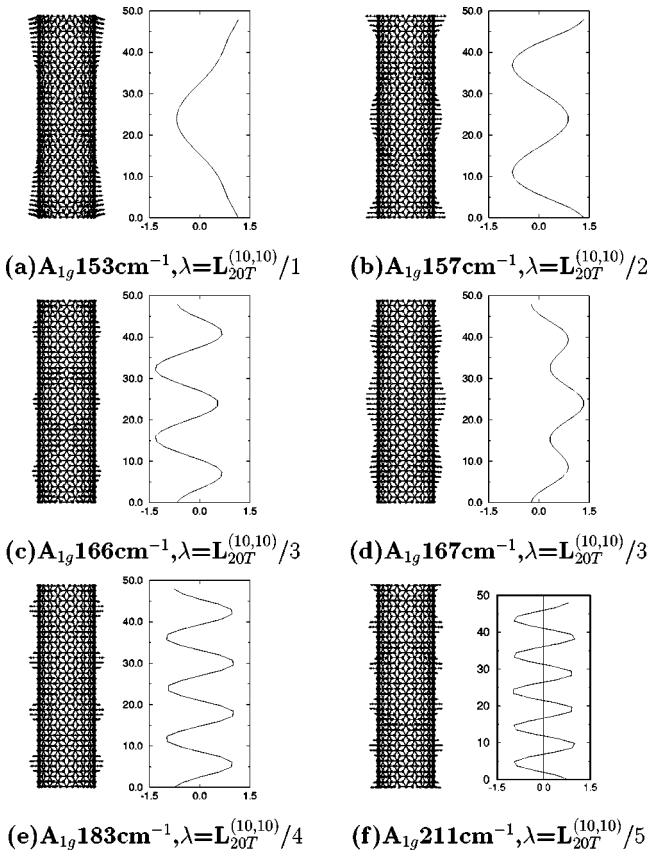

FIG. 2. Displacements for r breathing modes for a $20T$ (10,10) nanotube. The graphs shows the amplitude of the vibration as a function of the position of carbon atoms along the nanotube axis.

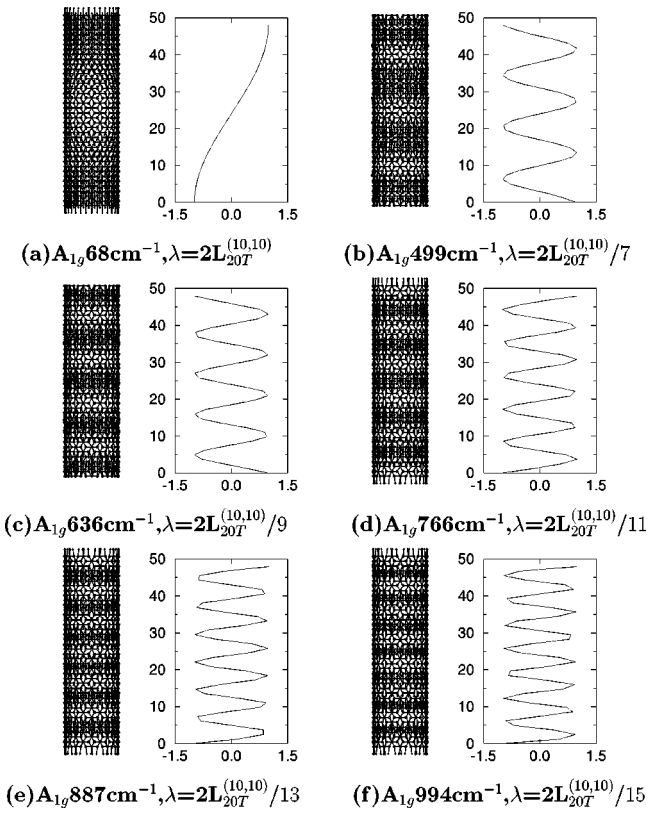

FIG. 3. Displacements for z breathing modes for a $20T$ (10,10) nanotube.

correspond to the r breathing modes, and those at 68, 499, 636, 766, 887, and 994 cm^{-1} correspond to the z breathing modes. The reason why we get several Raman-active modes is the symmetry-lowering effect associated with the finite tube length. In fact, we can see standing waves associated with the vibrations for the open ends in which the amplitude of vibration gives a local maximum at the ends.

In Figs. 2 and 3 we show the r and z breathing modes for several standing waves, respectively. In the figures we also show plots of the amplitude of the vibration as a function of the z coordinate of the atoms. In the Raman-active r breathing modes, the atoms at both ends of the nanotube move in the same phase ($+r$ and $+r$), while in the z breathing modes, the atoms at both ends move out of phase ($+z$ and $-z$). This is a symmetry requirement for the vibration, in which all Raman-active vibrations should have displacements corresponding to the second-rank tensor (x^2+y^2, z^2). Thus the wavelength for the standing waves becomes $20T/n$, and $20T\times 2/(2n-1)$ for the r and z breathing modes, respectively, where $n=1,2,3,\ldots$. The corresponding values of n for the r breathing modes at 153, 157, 166, 167, 183, and 211 cm^{-1} are $n=1$, 2, 3, 3, 4, and 5, respectively. The values of n for the z breathing modes at 68, 499, 636, 766, 887, and 994 cm^{-1} are $n=1$, 4, 5, 6, 7, and 8, respectively. When n becomes large, the positive and negative polarizations due to the standing wave cancel each other, and thus the Raman intensity becomes small.

It is noted here that the modes at 166 and 167 cm^{-1} are a mixture of $n=1$ and $n=3$ standing waves in which the two standing waves superimpose in the opposite and same phase, respectively, so that the amplitude of this vibration is perturbed. Since the r-breathing mode for an infinite nanotube has a large intensity at 165 cm^{-1}, the 167 cm^{-1} modes also show a large intensity. It is because of this coupling that the positive and negative amplitudes do not cancel each other's polarizations. Furthermore, we can see the coupling between the r-breathing and z-breathing modes in the 153 cm^{-1} and 224 cm^{-1} modes. In fact, the mode displacement vectors for the 153 cm^{-1} mode are tilted from the horizontal direction at the ends as is shown in Fig. 2(a). The mixed A_{1g} modes can be seen both in VV and VH configurations of Fig. 1.

Next we explain the Raman-active z breathing modes. The lowest-frequency z breathing mode appears at 68 cm^{-1} for a 49-Å length nanotube and the intensity is calculated to be even larger than for the 167 cm^{-1} mode. Since the frequency depends on the length, this mode becomes an acoustic mode with 0 cm^{-1} in the limit of an infinite length nanotube. If we can prepare short nanotubes with the same common lengths, we should be able to easily observed this mode. It is important to observe the standing wave using nanotubes with larger n since the frequencies are expected to occur in the intermediate frequency region. Although the expected intensity is weak, there should be no other Raman-active mode near this frequency, and for this reason, it should be relatively easy to find the standing wave in the spectra.

We think that the experimental peaks observed in the intermediate frequency range are associated with this standing

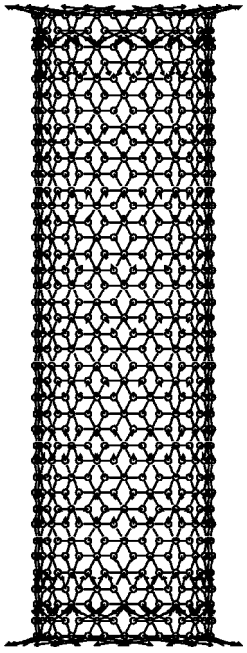

FIG. 4. Displacements for the phonon edge state mode for a 20T (10,10) nanotube.

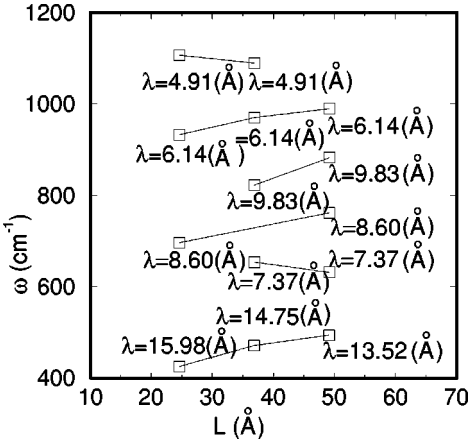

FIG. 5. The length dependence of the intermediate frequencies for (10,10) nanotubes. We connect similar vibrational wavelengths for different lengths of nanotubes.

wave mode. When the nanotubes exist in the form of ropes, the vibration is not so complicated because the coupling between nanotubes is very weak. Since the internanotube interaction should be on the order of 10 to 100 cm^{-1}, this interaction would be expected to perturb the lower Raman frequency modes. When we look at the vibration shown in Fig. 3, we see that only a small part of the vibration contributes to the net polarization. Thus if we have a free end of a nanotube, we should be able to observe the local z vibration which has a Raman intensity in the intermediate-frequency range.

When we look at the other Raman-active modes, we find interesting edge modes at 1217 cm^{-1} as shown in Fig. 4. This mode is an edge state of the r breathing mode in which a vibrational amplitude appears only at the two ends. This frequency does not depend on the length of the nanotube. In the electronic structure calculation of finite graphene sheets, it is known that there is an edge state for π bonding, which appears near the zigzag edges of graphite at the Fermi level.[13] This phonon mode corresponds to the phonon edge states that appear even at the armchair edges. If the nanotube has an open end, the intermediate frequency Raman peaks of the edge states should be observable experimentally. Although we did not try to calculate the phonon modes for the closed cap, we think that the corresponding edge Raman modes appear in a different frequency region. One possible frequency is the Raman frequency for the fullerenes, and the Raman-active modes for fullerenes have been calculated for the well-known C_{60} and C_{70} molecules. The characteristic Raman modes depend much on the shape and size of the fullerene. Thus it may be difficult to observe Raman modes associated with edge states for nanotube caps unless the shape of the cap is the same for the same chirality. It is known in graphite, however, that graphite defects give rise to a broad Raman peak around 1350 cm^{-1}. It is likely that the cap states will appear in the same region.

In Fig. 5 we plot the intermediate Raman frequencies for (10,10) nanotubes for different lengths of nanotube $L=5$, 10, and 20T. The number of nodes n for the same frequency region is different for different lengths L. When we connect a similar vibrational wavelength in the standing waves for different lengths of nanotubes, we get similar frequencies. The calculated frequencies increase or decrease with increasing L for a very small length, which reflects the discrete values of the wave vector along the nanotube axis and the phonon dispersion relations of infinite nanotubes in the intermediate-frequency region. Since the change of the frequency as a function of L is small compared with the diameter dependence of the r breathing modes, we therefore expect that the frequency change will be small for larger lengths of carbon nanotubes. The observed low intensity Raman peaks in the intermediate frequency range is determined by the finite wavelength of the local structure in a long nanotube. This might be one reason why we observe low-intensity peaks experimentally.

When we compare the Raman spectra for the 20T nanotube with those of 10T or 5T nanotubes, there is almost no dependence of the relative intensity of the intermediate-frequency modes with respect to the low-frequency A_{1g} modes. On the other hand, the absolute intensity for these modes is proportional to the nanotube length. This is because both low and intermediate frequencies correspond to long wavelength comparable to the length of nanotube and that the Raman intensities of both low and intermediate frequencies are proportional to the number of atoms within the bond polarization theory. We expect that the z breathing Raman intensity will appear for the infinite nanotube if the nanotube is bent since there should be no cancellation of the polarization for the vibration along nanotube axis. This may contribute to the enhancement of the Raman intensity for the intermediate modes.

IV. SUMMARY

In summary, our calculations predict the observation of Raman-active modes in finite-length carbon nanotubes in the

intermediate frequency region between 500 and 1200 cm^{-1}, associated with z-axis breathing modes. Standing waves associated with the r and z breathing modes are predicted at many Raman frequencies for finite-length nanotubes, and these results are consistent with the many weak peaks that are observed experimentally. We also found an edge phonon state that is Raman active in the r breathing mode, with a frequency that is independent of the length of the nanotube. Though most of the intermediate Raman frequencies depend on the length of the nanotube, some local structure in a long nanotube may give rise to intensity peaks in the experiments.

ACKNOWLEDGMENTS

The authors thank Dr. H. Kataura for stimulating discussions. R.S., G.D., and M.S.D. thank the International Joint Research Program of the New Energy and Industrial Technology Organization (NEDO), Japan, for its support. Part of the work by R.S. was supported by a Grant-in-Aid for Scientific Research (Grant No. 10137216) from the Ministry of Education and Science of Japan. The MIT work was partly supported by the NSF (Grant No. DMR 98-04734).

[1] S. J. Tans, R. M. Verschueren, and C. Dekker, Nature (London) **393**, 49 (1998).

[2] R. Saito, T. Takeya, T. Kimura, G. Dresselhaus, and M. S. Dresselhaus, Phys. Rev. B **57**, 4145 (1998).

[3] A. Kasuya, Y. Sasaki, Y. Saito, K. Tohji, and Y. Nishina, Phys. Rev. Lett. **78**, 4434 (1997).

[4] M. A. Pimenta, A. Marucci, S. D. M. Brown, M. J. Matthews, A. M. Rao, P. C. Eklund, R. E. Smalley, G. Dresselhaus, and M. S. Dresselhaus, J. Mater. Res. **13**, 2396 (1998).

[5] M. A. Pimenta, A. Marucci, S. Empedocles, M. Bawendi, E. B. Hanlon, A. M. Rao, P. C. Eklund, R. E. Smalley, G. Dresselhaus, and M. S. Dresselhaus, Phys. Rev. Lett. (to be published).

[6] A. M. Rao, E. Richter, S. Bandow, B. Chase, P. C. Eklund, K. W. Williams, M. Menon, K. R. Subbaswamy, A. Thess, R. E. Smalley, G. Dresselhaus, and M. S. Dresselhaus, Science **275**, 187 (1997).

[7] M. S. Dresselhaus, G. Dresselhaus, and P. C. Eklund, *Science of Fullerenes and Carbon Nanotubes* (Academic Press, New York, 1996).

[8] R. Saito, G. Dresselhaus, and M. S. Dresselhaus, *Physical Properties of Carbon Nanotubes* (Imperial College Press, London, 1998).

[9] T. Guo, C.-M. Jin, and R. E. Smalley, Chem. Phys. Lett. **243**, 49 (1995).

[10] A. Thess, R. Lee, P. Nikolaev, H. Dai, P. Petit, J. Robert, C. Xu, Y. H. Lee, S. G. Kim, A. G. Rinzler, D. T. Colbert, G. E. Scuseria, D. Tománek, J. E. Fischer, and R. E. Smalley, Science **273**, 483 (1996).

[11] C. Journet, W. K. Maser, P. Bernier, A. Loiseau, M. Lamy de la Chapelle, S. Lefrant, P. Deniard, R. Lee, and J. E. Fischer, Nature (London) **388**, 756 (1997).

[12] R. A. Jishi, L. Venkataraman, M. S. Dresselhaus, and G. Dresselhaus, Chem. Phys. Lett. **209**, 77 (1993).

[13] K. Nakada, M. Fujita, G. Dresselhaus, and M. S. Dresselhaus, Phys. Rev. B **54**, 17 954 (1996).